A Coupling of Empirical Explosive Blast Loads to ALE Air Domains in LS-DYNA®

Todd P. Slavik

Livermore Software Technology Corporation

Livermore, California, U.S.A.

Summary

A coupling method recently implemented in LS-DYNA® allows empirical explosive blast loads to be applied to air domains treated with the multi-material arbitrary Lagrangian-Eulerian (ALE) formulation. Previously, when simulating structures subjected to blast loads, two methods of analysis were available: a purely Lagrangian approach or one involving the ALE and Lagrangian formulations coupled with a fluid-structure interaction (FSI) algorithm. In the former, air blast pressure is computed with empirical equations and directly applied to Lagrangian elements of the structure. In the latter approach, the explosive as well as the air are explicitly modeled and the blast wave propagating through the ALE air domain impinges on the Lagrangian structure through FSI. Since the purely Lagrangian approach avoids modeling the air between the explosive and structure, a significant computational cost savings can be realized – especially so when large stand-off distances are considered. The shortcoming of the empirical blast equations is their inability to account for focusing or shadowing of the blast waves due to their interaction with structures which may intervene between the explosive and primary structure of interest. The new method presented here obviates modeling the explosive and air leading up the structure. Instead, only the air immediately surrounding the Lagrangian structures need be modeled with ALE, while effects of the far-field blast are applied to the outer face of that ALE air domain with the empirical blast equations; thus, focusing and shadowing effects can be accommodated yet computational costs are kept to a minimum. Comparison of the efficiency and accuracy of this new method with other approaches shows that the ability of LS-DYNA® to model a variety of new blast scenarios has been greatly extended.

Keywords: explosive, blast, ALE, coupling

1 Introduction

Increased simulation activities in the area of explosive air blast since the terrorist attacks of September 11th, 2001 have provoked major development efforts in the blast modeling capabilities of LS-DYNA®. Specifically, extensions of the empirical blast models originally implemented as *LOAD_BLAST appear in Version 971 Revision R4 as *LOAD_BLAST_ENHANCED. One of these enhancements makes it possible to apply empirical blast loads directly to the elements of an ALE air domain.

When faced with the task of simulating an air blast against a structure the analyst has at his disposal a variety of techniques available in LS-DYNA®. One commonly used approach involves explicit modeling of the air and explosive with the multi-material arbitrary Lagrangian-Eulerian (ALE) formulation in which appropriate equations of state are assigned to the materials and a burn model controls the explosive's detonation behaviour. The structure of interest is usually treated as Lagrangian and fluid-structure interaction (FSI) is used for communication between it and the ALE domain. The nature of explosive air blast involves a strong shock wave propagating through the air and accordingly the ALE elements must be small enough to capture the nearly discontinuous shock front. If long standoff, the distance from the explosive charge to the target structure, is of interest an enormous volume of air must be modeled. The result is a model of daunting proportions whose critical integration time step is dictated by the necessarily small air elements.

Another commonly used approach involves applying pressures due to the air blast directly to the Lagrangian structure. The blast pressure is computed with well calibrated empirical equations of *LOAD_BLAST which were derived using a compilation of results from thousands of explosive air blast experiments. In this approach there is no need to model the air or explosive since the required input for the empirical equations consists simply of the explosive charge weight and its position relative to the structure. Computational cost is typically orders of magnitude less than the equivalent ALE simulation. The restriction of this otherwise attractive method is that a clear line of sight must exist between the charge and the target structure. That is to say, shadowing of the blast wave due to the presence of intervening structures, or perhaps parts of the target structure shadowing itself, are not accounted for by the empirical blast equations. Another phenomenon not accommodated is the focusing of blast wave energy which occurs when waves merge after reflecting off structures.

Presented in the sequel is a new *LOAD_BLAST_ENHANCED feature which permits the empirical blast loads to be applied to an ALE air domain; in essence a marriage of the two aforementioned methods. With this technique only the air immediately surrounding the target structure is modeled with an ALE domain. If intervening structures are present the air domain is extended as necessary to enclose them. Blast pressures provided by the empirical laws are applied to a layer of ALE elements which face the explosive charge and act as a source for the adjoining air elements. Subsequently, on its own accord, the blast wave propagates through the remaining air domain eventually to impinge on the structure. In this way, the strengths of each method are preserved and combined to yield a new simulation technique which allows long standoffs to be studied without modeling copious air volumes while still retaining the ability to address shadowing and focusing. The implications of such a capability are significant as a new realm of air blast modeling possibilities now exist with LS-DYNA®. This purpose of this paper is to provide details of implementation of this feature, illustrate its use in the simulation environment, and compare results from it to other methods of simulating air blast loads on a structure.

2 Characteristics and Modeling of Blast Waves

An explosion in air creates a spherical shock wave which travels outward from the burst point with diminishing velocity. The free-air pressure at the shock front is termed the peak *incident pressure*. Air pressure decays after passage of the shock front and in its wake air particles traveling at a velocity less than that of the shock front form the *blast wind*. As this blast wave system expands into ever increasing volumes of atmosphere the pressure at the shock front decreases and the duration of the pressure pulse increases.

The form of the *incident blast wave* from the explosion of a spherical charge in air is shown in Figure 1 where P_o is the ambient atmospheric pressure and P_I is the peak incident pressure. The arrival time of the shock front is t_a and the *positive phase* of the blast wave extends to time t_+.

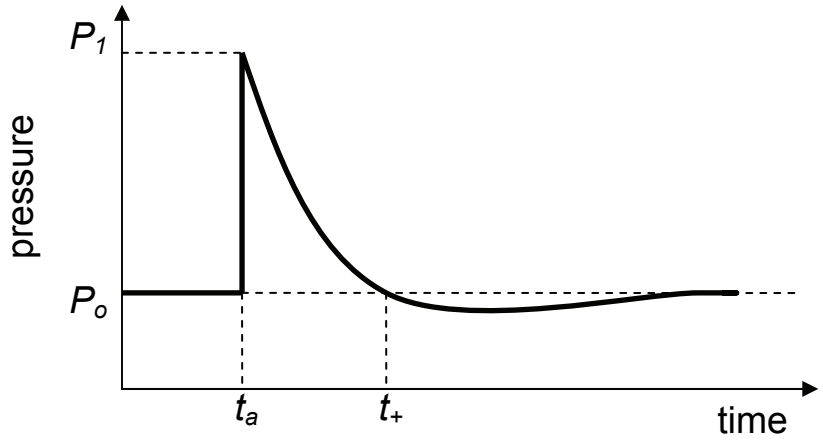

Figure 1: Incident blast wave pressure-time variation.

The functional form of the *Friedlander equation* serves as the basis for empirical modeling of the incident pressure time variation given by

$$P_{inc} = P_s(1-\tau)e^{-\alpha\tau} \tag{1}$$

where the decay parameter *α* and *peak overpressure*, defined as

$$P_s \equiv P_1 - P_o \tag{2}$$

depend on the *scaled range* given by

$$Z = R/W^{1/3} \tag{3}$$

where *R* is the distance from the charge center to the point of interest in the air and *M* is mass of the charge. The non-dimensional time is computed as

$$\tau = \frac{t - t_{bo} - t_a}{D_P} \tag{4}$$

where t_{bo} is a user-specified shift in time and the duration of the overpressure phase is given by

$$D_P = t_+ - t_a \tag{5}$$

The *negative phase* of the blast wave, when pressure drops below the ambient pressure, is present only at distances typically greater than about ten charge radii and is accommodated by the Friedlander equation.

When the shock front encounters an unyielding surface at normal incidence the motion of the air particles is abruptly terminated. Consequently a new reflected shock moving in the opposite direction results and due to the great compressibility of air the *reflected pressure* P_r at this front lies in the range

$$2P_1 \le P_r < 13P_1 \tag{6}$$

depending on the strength of the shock. The reflected pressure is also treated with the Friedlander equation, using a different decay parameter *β*, to give the relationship

$$P_{ref} = P_r(1-\tau)e^{-\beta\tau} \tag{7}$$

When a blast wave impinges on a surface at non-normal incidence an effective pressure comprised of incident and reflected pressure components is applied to the surface. This effective pressure is computed in the following manner

$$P_{eff} = P_{inc}\left(1 + \cos\theta - 2\cos^2\theta\right) + P_{ref}\cos^2\theta \tag{8}$$

where the *angle of incidence θ* is formed by the line from the charge center to the point of interest on the structure and the normal vector of the structure's surface at that point.

The *effective impulse* of the blast wave is computed as the time-integrated area under the effective overpressure curve by

$$I_{eff} = \int_{t_a}^{t_+} P_{eff}\, dt \tag{9}$$

and is of particular interest since it represents perhaps the most important aspect of the damage-causing ability of the blast. Further details on the empirical models underlying *LOAD_BLAST_ENHANCED can be found in References [1] and [2].

3 Description of Air Blast Test Model

A test model based on the work of Mullin and O'Toole [3] was used as the basis for comparison of various air blast simulation techniques. Shown in Figure 2 is a 517.1 gram spherical charge of TNT explosive of radius 4.28 centimeters. Also shown is a plate measuring 50 cm by 100 cm with mass four kilograms which represents the face of ballistic sled test apparatus. Motion of the sled is permitted only in the x-direction. At a standoff distance of 26.14 cm the charge is centered in front of the plate. The blast physics associated this arrangement presents several challenges to the simulation method. In particular, the angles of incidence range from zero at the center of the plate to nearly 65 degrees at the corners. Also, due to relatively short standoff, gases resulting from the explosion reaction process impinge the plate in addition to air particles so in a strict sense this is not purely air blast. The primary response quantity used for comparing the simulation results is the peak velocity attained by the plate since this relates directly to the force impulse imparted by the blast. Additionally, pressure is monitored at two locations on the plate: one at its center, referred to as Sensor #1, and the other, referred to as Sensor #2, offset five centimeters in each direction from a corner. From these pressure histories effective impulses for those points on the plate can be computed in accordance with Eqn. (9).

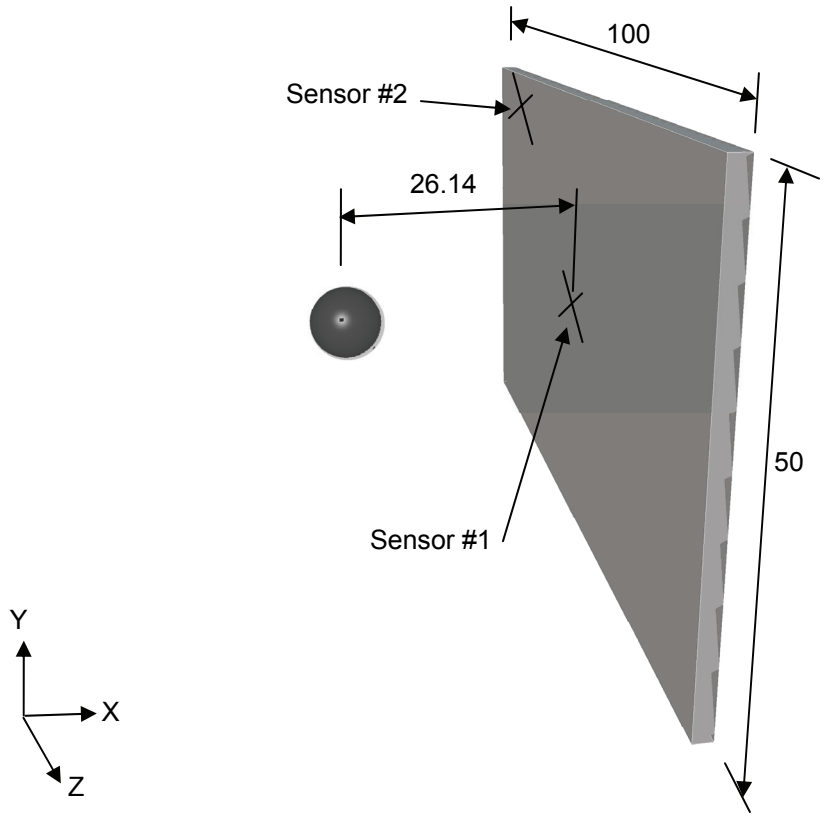

Figure 2: Test model of ballistic sled apparatus.

4 Empirical Blast Load Applied to Lagrangian Plate

Insofar as the empirical blast load approach stems from the reduction of a vast amount of experimental data and has been applied successfully for decades in various blast analyses it was deemed, for the purpose of this paper, an appropriate standard by which to judge other methods. To this end, a model consisting solely of a rigid plate comprised of square Lagrangian shell elements was developed to establish baseline response of the system described in Section 3. The plate was appropriately constrained to allow motion in only the x-direction and its elements had a side length of 2.5 millimeters. Following are the pertinent keywords used to define the blast.

```
*LOAD_BLAST_ENHANCED
$      bid         m        xbo        ybo        zbo        tbo       unit      blast
         1     517.1     -26.14        0.0        0.0        0.0          4          2
$      cfm       cfl        cft        cfp
       0.0       0.0        0.0        0.0
*LOAD_BLAST_SEGMENT_SET
$      bid      ssid     alepid
         1         1          0
```

Figure 3: Keyword input defining the empirical blast load.

The simulation was run to a time of 600 microseconds which required a mere 52 seconds of CPU time on a Linux-based workstation. Tabulated below are the response quantities, previously mentioned in Section 3, used to characterize the response. The effective impulses were computed from pressure-time histories recorded in the binary database *DATABASE_BINARY_BLSTFOR.

Plate Velocity (meters/second)	Impulse, Sensor #1 (Pascal-seconds)	Impulse, Sensor #2 (Pascal-seconds)
101	2220	326

Table 1: Response results for empirical blast approach.

5 ALE Air and Explosive Interacting with Lagrangian Plate

5.1 Description of Computational Model

Depicted in Figure 4 is a model developed for the purpose of establishing a baseline in which the air and explosive are explicitly treated with the ALE method. Hexahedral elements having an aspect ratio of unity comprise the ALE computational domain and employ the multi-material element ALE formulation with a second order advection scheme. The uniform rectilinear ALE mesh extends approximately five centimeters beyond the plate's edges in both the y and -z directions. As well, in the x direction, about five centimeters of additional ALE mesh was included behind the plate to accommodate its motion. An eighth-symmetric model is had by imposing appropriate boundary conditions to the nodes lying on the x-y, y-z and x-z planes which intersect at the charge center while non-reflecting boundary conditions are applied to the remaining exterior surfaces of the domain. The plate is modeled with rigid Lagrangian shell elements possessing only one free degree of freedom in the x-direction. An obvious mesh-biasing consequence arises when a rectilinear mesh is used for the calculation of spherical wave phenomena. A majority of LS-DYNA® user's are apt to apply this approach so it was done intentionally here to demonstrate the appropriateness of the method.

The air is treated as an ideal gas using the linear polynomial equation of state (EOS) while the Jones-Wilkins-Lee EOS is used to characterize the explosive. The charge is point detonated at its center with a programmed burn model. Initially the entire ALE mesh is occupied only by air but at the start of the calculation the explosive charge is represented by appropriately initializing the volume fractions of the elements enclosed by its spherical shape. Fluid-structure interaction between the ALE and Lagrangian parts is accomplished with a penalty based method. At the end of this section in Figure 5 in are some of the more salient LS-DYNA® keywords used in the ALE model.

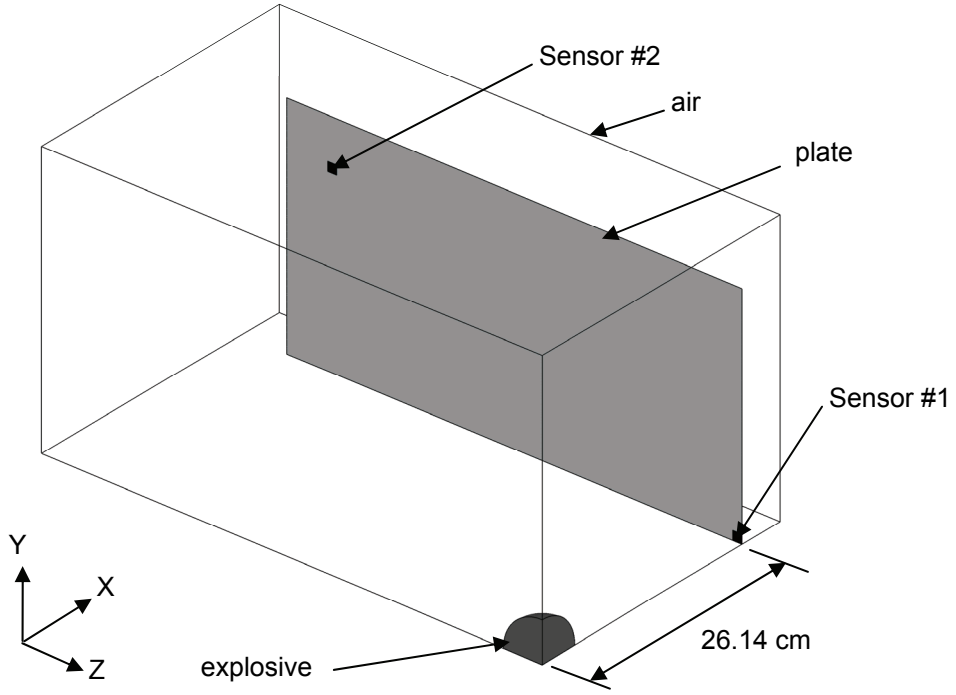

Figure 4: Eighth-symmetric model of ALE air and explosive interacting with Lagrangian plate.

5.2 Mesh Convergence Study

Mesh convergence was addressed with a series of calculations in which the size of the ALE elements was increasingly reduced with a refinement ratio of 1.6. In this study the size of the square elements of the plate was fixed at 2.5 mm. Specifics of the meshes and resulting response quantities are presented in Table 3 where CPU timing is given for the workstation described in Section 4. All simulations were run to 600 microseconds.

Element Size (mm)	Plate Velocity (m/sec)	Impulse, Sensor #1 (Pa-sec)	Impulse, Sensor #2 (Pa-sec)	ALE element count	CPU time (hours)
10.24	87.7	1731	307	50,220	0.2
6.4	90.3	1918	270	198,058	0.7
4.0	91.1	1958	294	807,300	3.4
2.5	92.1	1971	322	3,300,000	19.6

Table 2: Mesh details and simulation results from models used in ALE mesh convergence study.

As in Roache [4], the convergence rate exponent p for a mesh triplet is computed by

$$p = \log\left[\left(F_1 - F_3\right)/\left(F_1 - F_2\right)\right]/\log\left(r\right)$$

where F_i is the response quantity of interest, in this case plate velocity, for the i^{th} mesh and r is the mesh refinement ratio. The convergence rate exponent for the three coarsest meshes, found to be 3.01, is an indicator of a non-converged solution for a code such as LS-DYNA® which is at best second-order (p =2) accurate. Considering the three finest meshes we find p=1.25, an indication the triplet may be in the asymptotic convergence regime, and from this the *estimated numerically exact solution* F_o for plate velocity is computed with

$$F_o = F_1 + \left(F_1 - F_2\right)/\left(r^p - 1\right)$$

which yields the value F_o=93.4 meters/second. Under these circumstances the 4mm mesh exhibiting about 2.5% relative error from the estimated numerically exact solution was deemed appropriate for the present work.

```
*PART
$    title
air domain
$      pid       sid       mid     eosid
         1         1         1         1
*SECTION_SOLID
$      sid    elform
         1        11
*MAT_NULL
$      mid        ro        pc
         1  0.001225  -1.0e+05
*EOS_LINEAR_POLYNOMIAL
$#   eosid        c0        c1        c2        c3        c4        c5        c6
         1                                                0.4       0.4
$       e0        v0
 2.575e-06       1.0
*PART
$    title
explosive
$      pid       sid       mid     eosid
         0         1         2         2
*MAT_HIGH_EXPLOSIVE_BURN
$      mid        ro         d       pcj      beta         k         g      sigy
         2     1.570     0.693     0.210
*EOS_JWL
$    eosid         a         b        r1        r2      omeg        e0        vo
         2     3.712   0.03231      4.15      0.95      0.30      0.07       1.0
*SECTION_SOLID
$#   secid    elform       aet
         2        11
*CONTROL_ALE
$      dct      nadv      meth      afac
         0         1         2        -1
$#   start       end     aafac     vfact      prit       ebc      pref   nsidebc
       0.0       0.0       0.0       0.0       0.0         0  1.030e-6
*CONSTRAINED_LAGRANGE_IN_SOLID
$#   slave    master     sstyp     mstyp     nquad     ctype     direc     mcoup
         3         1         1         1         0         4         2
$#   start       end      pfac      fric    frcmin      norm   normtyp      damp
       0.0       0.0        -1       0.0       0.0         0         0         0
$#      cq      hmin      hmax     ileak     pleak   lcidpor     nvent  blockage
       0.0       0.0       0.0         0       0.0         0         0         0
*DEFINE_CURVE
$#    lcid      sidr       sfa       sfo      offa      offo    dattyp
         1
$#                a1                  o1
                  0.0                 0.0
                0.025               3.e-5
```

Figure 5: Keyword input pertaining to the ALE features (centimeter-gram-microsecond unit system).

6 Empirical Blast Load Applied to ALE Air Interacting with Lagrangian Plate

6.1 Development and Implementation of Coupling Method

Central to the method of coupling the empirical blast loads to an ALE domain is special ALE element formulation referred to as an ambient element. Although somewhat of a misnomer the element type falls into this category within the framework of LS-DYNA®. In practice a single element layer of this ALE ambient formulation makes up the exterior surface of the air domain which faces the blast. Its

function is to receive information from the blast equations then convert it to thermodynamic state data which is subsequently applied as a source to adjoining ALE air elements.

Within the context of the ideal gas law the pressure and density suffice the describe the thermodynamic state of the air, hence, the incident pressure from the blast is straightforwardly prescribed at the quadrature point situated at the center of the ambient element. The density of the air is computed for the element's quadrature point in the following manner.

When shocked from ambient atmospheric density ρ_o the density of the air at the shock front ρ_1 is obtained from the Rankine-Hugoniot jump discontinuity relation (see Reference [6])

$$\frac{\rho_1}{\rho_o} = \frac{6(P_1/P_o)+1}{(P_1/P_o)+6} \tag{10}$$

and when treated as an ideal gas the density ρ of the air after passage of the shock front follows the isentropic relation

$$\rho = \rho_1 \left(\frac{P_{inc} + P_o}{P_1} \right)^{1/\gamma} \tag{11}$$

What remains to be determined, in order to completely describe the flow conditions of the blast wave system, is the velocity of the air particles in the blast wind. Appealing again to the Rankine-Hugoniot relations the particle velocity at the shock front u_p is found with

$$\left(\frac{u_p}{C_o} \right)^2 = \frac{25(P_1/P_o - 1)^2}{42(P_1/P_o)+7} \tag{12}$$

where C_o is the sound speed in air before arrival of the shock. The relations (10) and (12) are valid for an ideal gas with specific heat ratio of $\gamma = c_p/c_v = 1.4$..

Next the *dynamic pressure* at the shock front is computed as

$$Q_s = \frac{1}{2}\rho_1 u_p^{\,2} \tag{13}$$

and decay of the dynamic pressure follows the functional form

$$Q = Q_s(1-\zeta)e^{-\varphi\zeta} \tag{14}$$

where ζ is time normalized by the positive phase duration of the of the particle velocity D_u and φ is a decay parameter. Finally, combining equations (11), (13) and (14) along with the following yields a means for determination of the particle velocity u of the blast wind

$$Q = \frac{1}{2}\rho u^2 \tag{15}$$

The velocity computed in Equation (15) is for the particles at the center of the ambient element segment so it is subsequently distributed to the nodes of the element in an area-weighted fashion.

6.2 Application of Coupling Method

The new coupling method was exercised in the model shown in Figure 6. Here, not unlike in the model of Section 5, the plate is surrounded by an ALE air domain and FSI handles communication between them. Notably discernable, however, are the diminished size of the ALE domain, which now extends only 10 cm from the plate towards the charge, and the absence of the explosive modeled by ALE elements - the spherical charge depicted in the figure is for illustrative purposes only and does not enter into the calculation. A one-element thick layer of ALE ambient elements is situated on the side of the air domain facing the charge. To enforce conditions of quarter-symmetry flow constraints were imposed in an appropriate manner on nodes of the x-y and x-z planes whose line of intersection pass through the charge origin. All other exterior surfaces of the air domain were treated as non-

reflecting boundaries. The ALE and ambient elements were hexahedral with perfect aspect ratio and side length of 4 mm. Square elements measuring 2.5 mm were used in the plate.

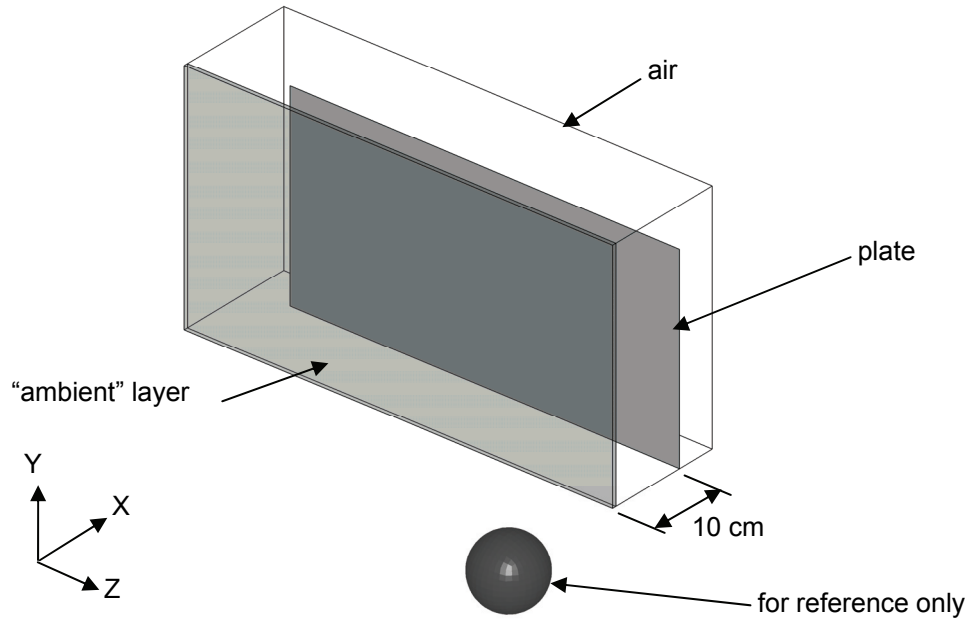

Figure 6: Model used to exercise the new coupling method.

Definition of the blast source and ambient layer part through keyword input can be found in Figure 7. The simplicity of using this new feature is surprisingly simple. First, it should be noted that both the ambient elements and ALE elements of the air domain must use element formulation #11 (ELFORM=11) as well as the same equation of state type #1 (*EOS_LINEAR_POLYNOMIAL) made to function as the ideal gas law. Activation of the ambient formulation's special properties is accomplished by setting AET=5 in *SECTION_SOLID. Next, the exterior segments of the ambient layer are identified with *LOAD_BLAST_SEGMENT and in this keyword the parameter ALEPID must match the part number of the ambient elements. The blast is defined in a manner identical to that used in Section 4, except here a particularly powerful feature is exploited. The use of a negative time offset TBO of 30 microseconds arranges for the blast wave to imminently strike the ambient layer at the start of the calculation - computational cost savings is immediately afforded by inclusion of this feature since it permits a 600 microsecond event to be simulated in 570 microseconds. In this way computation time is not expended waiting for the arrival of wave whose character is known *a priori*.

```
*PART
$# title
ambient layer
$#     pid     secid       mid     eosid      hgid      grav    adpopt      tmid
         2         2         1         1
*SECTION_SOLID
$#   secid    elform       aet
         2        11         5
*LOAD_BLAST_SEGMENT_SET
$      bid      ssid    alepid
         1         1         2
*LOAD_BLAST_ENHANCED
$      bid         m       xbo       ybo       zbo       tbo      unit     blast
         1     517.1    -26.14       0.0       0.0      -30.         4         2
$      cfm       cfl       cft       cfp
       0.0       0.0       0.0       0.0
```

Figure 7: Keywords used in applying empirical blast to ALE ambient elements.

Results from the coupled simulation compared with those from the methods of Section 4 and 5 are tabulated below. In parentheses appear the differences in response relative to the empirical approach. Lower plate velocity is seen in both the coupled and ALE simulations. Most likely responsible for this are loss mechanisms inherent in the ALE scheme, namely, the dissipation due to advection and the necessary application of artificial bulk viscosity which consumes energy and smears the shock front. Further, although particular attention was focused on controlling leakage at the FSI interface, a certain amount is unavoidable and accounts for some reduction in momentum transferred to the plate. Next noted is that the plate in the coupled simulation attains a higher velocity than that in the pure ALE simulation. Again, the effects of dissipation and smearing are culprit since in the coupled case the shock front experiences less attenuation as it traverses less mesh. Upholding this as well is the stronger impulse at Sensor #1 in the coupled approach whereas at Sensor #2 it is lessened as a result of the shock having passed through more mesh. Lastly, as a direct consequence of the number of ALE elements being more than halved in the coupled model the computation time is roughly half that of the ALE simulation. Overall performance of the coupled method is outstanding both in its computational time savings and ability accurately capture the shock behaviour.

	Plate Velocity (m/sec)	Impulse, Sensor #1 (Pa-sec)	Impulse, Sensor #2 (Pa-sec)	ALE element count	CPU time (hours)
Coupled	94.5 (-6%)	2123 (-4%)	296 (-9%)	393,300	1.6
ALE 4mm	91.1 (-10%)	1958 (-12%)	294 (-10%)	807,300	3.4
Empirical	101	2220	326	n/a	0.01

Table3: Comparison of results with the empirical approach serving as the reference.

7 Conclusions

Presented is a method of coupling empirical blast loads to ALE domains which extends the capabilities of LS-DYNA® in the area of air blast simulation. The methodology underlying the empirical blast loads is widely accepted and the manner in which it was integrated into the ALE framework is based on sound scientific principles. In practice the new blast coupling feature is simple to activate using commonly known keywords. Not surprisingly, simulation of a ballistic sled with this new technique produced results which fell in line with results of the two parent methods which it couples. Similar accuracy and efficiency are expected when exercised in more challenging blast scenarios. In situations involving long standoff distances, a significant computational cost savings will be realized by relieving the burden of unnecessarily simulating the propagation of a shock wave as it travels unabated to its target.

8 References

[1] Randers-Pehrson, G. and K.A. Bannister, “Airblast Loading Model for DYNA2D and DYNA3D,” ARL-TR-1310, Army Research Laboratory, Aberdeen Proving Ground, MD, April 1997.

[2] Kingery, C.N. and G. Bulmash, “Air-Blast Parameters from TNT Spherical Airburst and Hemispherical Surface Burst,” ABRL-TR-02555, U.S. Army Ballistic Research Laboratory, Aberdeen Proving Ground, MD, April 1984.

[3] Mullin, M.J. and T.J. O’Toole, “Simulation of Energy Absorbing Materials in Blast Loaded Structures,” 8th International LS-DYNA Users Conference 2004, Dearborn, MI, 2004.

[4] Roache, P.J., “Verification and Validation in Computational Science and Engineering,” Hemosa Publishing, Albuquerque, NM, 1998.

[5] Logan R.W. and C.K. Nitta, “Comparing 10 Methods for Solution Verification, and Linking to Model Validation,” AIAA Journal of Aerospace Computing, Information, and Communication, 3: July 2006, pp. 354-373.

[6] Kinney, G.F. and K.J. Graham, "Explosive Shocks in Air," Springer-Verlag New York Inc., (ISBN: 0-540-15147-8), 1985.